نشریه ژئومکانیک و ژئوانرژی (ژئومکانیک نفت)
GEOMECHANICS and GEOENERGY JOURNAL (GGJ)

Original article

Thermal cycling effects on pile–soil–pile interaction in unrestrained energy pile groups: A THM numerical study

Marjan Sadrjamali[1], Amir Hamidi[1*], Abtin Rooz[2]

1- Department of Civil Engineering, School of Engineering, Kharazmi University, Tehran, Iran
2- School of Engineering, Deakin University, Waurn Ponds, Victoria, Australia

Received: 2026/03/28; Revised: 2026/05/29; Accepted: 2026/06/18

DOI: 10.22107/ggj.2026.600163.1273

Keywords

Energy piles,
Thermal cycling,
Pile group interaction,
Interaction factor,
Saturated clay,
Thermo-hydro-mechanical modelling

Abstract

Energy piles provide a sustainable solution for building heating and cooling while also serving as structural foundation elements. However, cyclic thermal loading can alter pile–soil interaction and affect the settlement response of surrounding structural piles, particularly in groups without pile-head restraint. This study investigates the thermo-hydro-mechanical response of unrestrained energy pile groups embedded in saturated clay, with emphasis on the interaction factor between thermally active piles and nearby structural piles. A three-dimensional numerical model was developed and verified against established thermal consolidation, single energy pile, and pile group case studies. The verified model was then used to examine the effects of pile diameter, length, spacing, and group size under two repeated thermal cycles. The results reveal a clear heating–cooling asymmetry, with greater thermal interaction during heating, indicating that pile expansion governed the maximum settlement interaction. During heating, the interaction factor was approximately 0.03–0.05, while during cooling it was lower, approximately 0.005–0.02. The geometrical variables acted in combination: increased spacing reduced pile-to-pile interaction, larger pile groups intensified the thermal influence, and longer piles reduced the interaction factor by about 61–68% during cooling and 47–52% during heating when pile spacing and diameter were kept constant. Heating generated compressive axial stresses in the energy piles, while cooling produced tensile stresses of comparable magnitude, highlighting the need to consider both phases in serviceability assessment. A simplified dimensionless expression is proposed for preliminary estimation of thermally induced settlement interaction in unrestrained energy pile groups.

1. Introduction

Energy piles are increasingly employed as multifunctional foundation systems that combine structural load transfer with shallow geothermal heat exchange [1,2]. In these systems, heat-exchanger pipes are embedded within foundation piles, allowing the pile to operate both as a load-bearing element and as part of the building heating and cooling system. This dual function makes energy piles an attractive solution for reducing energy demand and supporting more sustainable infrastructure [3]. However, the repeated heating and cooling of piles introduces additional thermo-mechanical effects that are not normally considered in conventional pile design.

When an energy pile is heated, it tends to expand; when it is cooled, it contracts [4]. These temperature-induced deformations may modify axial stress, shaft resistance, pore-water pressure, and pile-head displacement [5]. In pile groups, the response becomes more complex because thermally active piles may influence nearby structural piles through the surrounding soil [6]. Fig. 1 schematically illustrates the thermal pile–soil–pile interaction mechanism in an unrestrained energy pile group under heating and cooling conditions. As a result, the serviceability performance of the foundation may be affected even when the ultimate geotechnical capacity is not critical [7]. Settlement interaction is therefore an important design consideration, particularly for structures where differential movement between piles must be limited [8].

Previous studies have shown that interaction factor approaches can be useful for assessing pile group settlement [9,10]. The interaction factor concept was originally developed for mechanically loaded pile groups and has later been adapted to energy pile groups [11]. However, most available interaction factor methods are mainly applicable to specific boundary conditions, especially pile groups with head restraints, raft connections, or fixed-head assumptions [12]. In practice, some pile groups may behave closer to unrestrained or free-head conditions, where the absence of a cap or strong head restraint allows thermal deformation to develop more freely. Under these conditions, the settlement interaction between thermally active and structural piles may differ from that observed in restrained systems.

Although numerical modelling has been widely used to study the behaviour of energy piles [13-15], several limitations remain in the available literature. Many studies focus on single piles [16], capped pile groups [17], or thermo-mechanical behaviour without fully addressing the combined thermo-hydro-mechanical response [18]. In addition, existing IF formulations are often geometry-specific, complex, or difficult to use in preliminary design. Some regression-based expressions require many coefficients and provide limited physical interpretation, which reduces their practical value for engineers.

This study investigates the thermo-hydro-mechanical response of unrestrained energy pile groups embedded in saturated clay. The main focus is the IF between thermally active piles and nearby structural piles under repeated heating and cooling cycles. The effects of pile diameter, pile length, pile spacing, and group size are examined using a verified three-dimensional numerical model. Based on the resulting numerical database, a simplified dimensionless expression is proposed for estimating thermally induced settlement interaction in unrestrained energy pile groups. The study aims to provide a more practical serviceability-based framework for evaluating pile-to-pile interaction under cyclic thermal loading.

2. Background and research gap

2.1. *Thermo-mechanical behaviour*

The behaviour of energy piles is governed by the interaction between thermal loading, mechanical loading, and the surrounding soil response [19]. During heating, the pile tends to expand, but this expansion is partly restrained by the soil and the pile-head boundary condition. This restraint can generate additional compressive stress within the pile [20]. During cooling, the pile contracts, which may lead to tensile stress development [21]. Therefore, cyclic temperature changes can produce repeated stress reversals, even when the applied mechanical load remains constant.

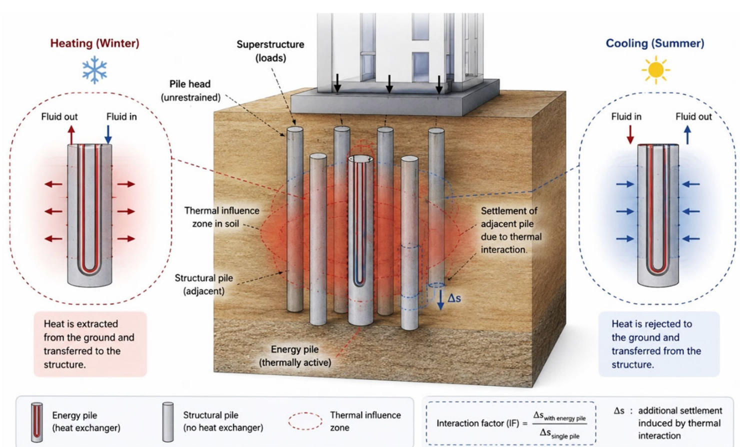

Fig. 1. Conceptual illustration of thermal pile–soil–pile interaction in an unrestrained energy pile group under heating (winter) and cooling (summer) conditions

Table 1. Governing equations employed in the coupled THM framework

Physical process	Governing equation	Eq. No.	Main variables	Description
Mechanical equilibrium	$\nabla.(D\varepsilon^e - pI) + \rho g = 0$	(2)	, ε^e, p, I, D ρ, g	It describes static equilibrium of the saturated porous medium by considering elastic strain, pore-water pressure, body force, and gravity.
Fluid mass conservation	$\frac{\partial p}{\partial t} - \frac{\partial T}{\partial t} + \nabla.u_{rf} + \nabla.u_s = 0$	(3)	, T, u_{rf}, p u_s	It represents pore-pressure generation, and dissipation caused by deformation, fluid flow, and temperature variation.
Thermal energy conservation	$c\frac{\partial T}{\partial t} + c_f u_{rf}.\nabla T - \nabla.(\Lambda \nabla T) = 0$	(4)	, c, c_f, T u_{rf}, Λ	It describes heat storage, heat conduction, and heat transfer associated with fluid movement.
Simplified heat conduction	$\rho c\frac{\partial T}{\partial t} - \nabla.(\lambda \nabla T) = 0$	(5)	, $\rho, c, \lambda T$	It is used when porosity variation and convective heat transfer are neglected, allowing heat transfer to be represented mainly by conduction.

The magnitude of thermally induced stress and displacement depends on several factors, including pile geometry, soil stiffness, pile–soil interface behaviour, drainage conditions, and the level of pile-head restraint. In saturated clay, thermal loading may also generate excess pore-water pressure because temperature changes affect the soil skeleton and pore fluid [22]. Positive pore pressures may develop during heating, while cooling may generate negative excess pore-water pressure [23]. These hydraulic effects influence the effective stress state and may contribute to the time-dependent settlement response of the pile group.

Previous numerical, analytical, laboratory, and field studies have improved understanding of energy pile behaviour [24]. However, a considerable portion of the literature has focused on single piles or pile groups with head restraint. The response of unrestrained pile groups has attracted comparatively limited attention, even though this condition is important for understanding the fundamental pile–soil–pile interaction caused by thermal loading. In free-head systems, thermal expansion and contraction may directly influence pile-head displacement, making settlement interaction a pivotal serviceability concern. Unlike regional geothermal mapping studies that use artificial intelligence or optimization methods to predict subsurface temperature distributions (e.g., [25-27]), the present study focuses on local-scale THM soil–structure interaction and serviceability settlement response of unrestrained energy pile groups.

2.2. *Interaction factor methods for pile groups*

The interaction factor is commonly used to describe the influence of one pile on the settlement response of another pile within a group. In conventional pile group analysis, the concept provides a simplified way to account for pile–soil–pile interaction under mechanical loading (e.g., [28-31]). This approach is attractive because it enables the complex group response to be expressed using a relatively simple coefficient.

For energy pile groups, the interaction factor concept has been extended to account for thermally induced displacement [32,33]. Interaction factor (*IF*) represents the settlement influence of a thermally active pile on an adjacent structural pile and can be expressed as:

$$IF = \frac{(\Delta s)_{adjacnt}}{(\Delta s)_{single}} \quad (1)$$

where $(\Delta s)_{adjacnt}$ is the additional settlement of a nearby structural pile induced by thermal loading of an energy pile, and $(\Delta s)_{single}$ is the reference settlement of a single pile under comparable conditions. This parameter is particularly useful for serviceability assessment because, while thermal loading may not govern ultimate capacity, it can still affect differential settlement, pile-head displacement, and load redistribution within the group.

However, application of conventional interaction factor methods to energy piles is not straightforward. Thermal loading produces expansion and contraction rather than only downward mechanical displacement. Moreover, heating and cooling phases may not have symmetric effects. The interaction factor may therefore depend not only on pile spacing and geometry, but also on the thermal phase, group configuration, and pile-head boundary condition. For this reason, interaction factors developed for mechanically loaded pile groups or restrained energy pile groups may not be directly applicable to unrestrained energy pile groups.

2.3. *Limitations of existing numerical and empirical approaches*

Although numerical modelling has become a common approach for analyzing energy piles, existing methods still have several limitations. First, many models are developed for a specific soil type, pile arrangement, and boundary condition (e.g., [34]). As a result, their findings may not be directly transferable to other foundation systems. This is particularly important for interaction factor formulations, which are often calibrated using a limited numerical database.

Second, some existing formulations for energy pile interaction are mathematically complex (e.g., [35]). High-order polynomial equations may reproduce numerical results within a specific calibration range, but they are difficult to interpret physically and inconvenient for practical design. A formulation with many coefficients may also create uncertainty when applied outside the original range of pile diameter, length, spacing, thermal loading, or group size.

Third, some numerical studies simplify the coupled nature of the problem (e.g., [36]). Energy pile behaviour in saturated soil is inherently thermo-hydro-mechanical because temperature change may influence deformation and pore-water pressure simultaneously. Ignoring one part of this coupled response may reduce the reliability of settlement predictions, especially in clayey soils where drainage and pore-pressure dissipation are important.

Fourth, many studies do not fully discuss numerical reliability, including mesh sensitivity, boundary effects, pile–soil interface assumptions, and model limitations (e.g., [37]). These factors can affect the calculated pile displacement and interaction factor. For serviceability-based assessment, where the magnitude of settlement may be relatively small, numerical accuracy and transparent assumptions are essential.

Fifth, since the present study is based on a controlled numerical parametric database rather than a sequential field database, automated database updating, dynamic filtering, and normalization of incoming monitoring data were outside the scope of this work.

Finally, the broader applicability of current models remains limited [38]. Regular two-year thermal cycles are useful for controlled parametric assessment, but real energy pile systems may experience irregular seasonal demand, variable heating and cooling amplitudes, groundwater flow, soil layering, creep, or long-term thermal accumulation. These factors should be recognized when interpreting numerical results and proposing simplified design expressions.

2.4. *Objectives and contribution of this study*

The objective of this study is to investigate the thermo-hydro-mechanical interaction between thermally active piles and nearby structural piles in unrestrained energy pile groups. The study focuses on saturated clay and examines the influence of pile geometry and group configuration on the interaction factor under cyclic heating and cooling.

The main contributions of the study are as follows:

- A three-dimensional thermo-hydro-mechanical numerical model is used to evaluate unrestrained energy pile groups under repeated thermal cycles .
- The model is verified against established thermal consolidation, single energy pile, and pile group case studies before being used for the parametric investigation .
- The effects of pile diameter, pile length, pile spacing, and group size are systematically examined for 3 × 3, 4 × 4, and 5 × 5 pile groups .
- The difference between heating and cooling phases is explicitly evaluated, allowing the thermal phase dependency of the interaction factor to be identified .
- A simplified dimensionless expression is proposed for estimating the interaction factor in

unrestrained energy pile groups within the calibration range of the numerical database.

Through these contributions, the study provides a practical basis for preliminary serviceability assessment of thermally induced settlement interaction in unrestrained energy pile groups. The proposed framework is not intended as a universal design equation, but as a calibrated framework for conditions similar to those analyzed in this study. Further validation is required for other soil types, pile-head restraints, groundwater conditions, and long-term operational conditions.

3. THM modelling framework

3.1. Governing equations

The response of energy piles embedded in saturated clay is governed by the coupled interaction between mechanical deformation, pore-fluid flow, and heat transfer. Therefore, the problem was treated as a thermo-hydro-mechanical (THM) process in which static equilibrium, fluid mass conservation, and thermal energy conservation were solved in a coupled manner. The governing equations applied in the numerical framework are summarized in Table 1.

where D is the elastic constitutive tensor, ε^e is the elastic strain tensor, p is pore-water pressure, I is the identity tensor, ρ is total mass density, g is gravitational acceleration, T is temperature, u_rf is the velocity of the fluid phase relative to the solid phase, u_s is the displacement vector of the solid phase, c is the equivalent heat capacity, c_f is the fluid heat capacity, Λ is the equivalent thermal conductivity tensor, and λ is the equivalent thermal conductivity.

For the energy pile simulations, the influence of porosity variation and convective heat transfer was neglected. Therefore, the simplified heat conduction equation was adopted together with the mechanical equilibrium and fluid mass conservation equations. These equations were solved over the same numerical model to capture the coupled response of pile deformation, pore-water pressure variation, and heat transfer during cyclic thermal loading.

3.2. Implementation of coupled THM analysis

The numerical analysis was performed using a three-dimensional finite element model. The coupled THM response was implemented by combining the mechanical deformation, pore-water pressure, and temperature fields within the soil–pile system. The model was designed to capture the interaction between thermal expansion or contraction of the energy piles, pore-water pressure variation in the saturated clay, and the resulting settlement response of adjacent structural piles.

The soil was modelled as a saturated porous medium, while the piles were represented as concrete structural elements embedded within the soil model. The pile–soil interface was included to allow load transfer between the pile and surrounding soil during mechanical loading and thermal cycling. Mechanical loading was applied to the pile heads to represent the structural load transferred from the superstructure. Thermal loading was then applied to the energy piles in the form of repeated heating and cooling cycles.

In the coupled analysis, temperature variation modifies the thermal strain of the pile and surrounding soil. This thermal strain affects the stress state and displacement field. At the same time, thermal loading in saturated clay can generate excess pore-water pressure due to the different thermal expansion and compressibility characteristics of the soil structure and pore fluid. The generated pore-water pressure then influences the effective stress and settlement response. Therefore, the THM framework enables the thermal, hydraulic, and mechanical responses to interact throughout the analysis rather than being treated as independent processes.

The modelling procedure consisted of three main stages. First, the initial geostatic condition was established to represent the in-situ stress state of the saturated soil. Second, the mechanical load was applied to the pile heads and maintained throughout the analysis. Third, cyclic thermal loading was applied to the energy piles while monitoring the displacement response of adjacent structural piles. The interaction factor was then calculated from the thermally induced settlement response and used to evaluate pile–soil–pile interaction under different geometrical and group configurations.

This implementation was therefore used as a coupled numerical framework rather than as a newly derived constitutive model, and its applicability was assessed through the verification and validation cases described in the following section.

3.3. Coupling strategy and numerical formulation

The behaviour of energy pile groups requires a coupled formulation since the governing physical processes are mutually dependent. The mechanical response controls deformation and variations in pore volume; the hydraulic response controls pore-pressure generation and dissipation; and the thermal response controls expansion, contraction, and heat transfer within the soil–pile system. These mechanisms are particularly important in saturated clay, where low permeability can delay pore-pressure dissipation and increase the time-dependent nature of settlement.

In the present framework, the equilibrium equation controls the stress and displacement field, the mass conservation equation governs pore-water pressure response, and the heat transfer equation controls temperature variation. These equations were solved over the same numerical model so that changes in one field could influence the others during each loading step. This approach is suitable for evaluating settlement interaction because the displacement of adjacent structural piles depends not only on direct mechanical loading but also on thermal strain and pore-pressure variation induced by nearby energy piles.

The energy piles were subjected to cyclic temperature variation to represent seasonal heating and cooling operation. During heating, pile expansion tends to increase compressive stress and outward displacement in the surrounding soil. During cooling, pile contraction can produce tensile stress and reverse the direction of thermally induced deformation. This cyclic stress reversal is central to the serviceability response of energy pile groups and is therefore explicitly considered in the numerical framework.

3.4. Assumptions and scope of applicability

The THM modelling framework was developed to investigate the fundamental settlement interaction between thermally active piles and adjacent structural piles in unrestrained pile groups. To keep the numerical database systematic and interpretable, several assumptions were adopted.

The soil was assumed to be homogeneous, isotropic, and fully saturated. The groundwater table was considered to be located at the ground surface, and groundwater flow was not explicitly modelled. Heat transfer was assumed to occur mainly by conduction, while convective heat transfer and long-term groundwater-induced thermal drift were neglected. The thermal loading was idealized as regular heating and cooling cycles, rather than irregular operational demand from a real building energy system.

The pile material was modelled as linear elastic concrete, and the pile temperature was applied uniformly along the thermally active pile elements. This assumption is commonly used in numerical studies where the main objective is to evaluate soil–pile interaction rather than the detailed performance of the heat-exchanger pipe system [39]. The circulation of heat-carrier fluid and the detailed pipe geometry were therefore not simulated.

The pile heads were treated as unrestrained to isolate the influence of thermal pile–soil–pile interaction without the additional stiffness contribution of a cap, raft, or rigid superstructure. As a result, the findings are most applicable to free-head or weakly restrained pile group conditions. They should not be directly transferred to fixed-head, capped, or piled-raft systems without further calibration.

In this context, soil–structure interaction is represented through the coupled pile–soil continuum and pile–soil interface response. The interaction between thermally active energy piles, surrounding soil, and adjacent structural piles is evaluated through the interaction factor, settlement response, axial stress variation, pore-water pressure response, and temperature distribution. The superstructure itself is not explicitly modelled, as the study focuses on local-scale pile–soil–pile interaction in unrestrained energy pile groups rather than full building–foundation interaction.

The proposed framework is therefore intended for preliminary serviceability assessment of thermally induced settlement interaction in unrestrained energy pile groups embedded in saturated clay. Its applicability is limited to conditions similar to those considered in the numerical model. Further validation is required before extending the results to layered soils, unsaturated soils, anisotropic ground conditions, irregular pile arrangements, long-term thermal accumulation, creep, freezing–thawing effects, or different pile-head restraint conditions.

3.5. Model verification and numerical reliability

Prior to conducting the parametric analyses, the numerical framework was assessed through a staged verification and validation procedure. The simulations were performed using Abaqus 2013, with a modified three-dimensional eight-node coupled element (C3D8PT) was implemented through the input file to represent the displacement, pore-pressure, and temperature fields required for thermo-hydro-mechanical analysis [40,41]. The soil was modelled as a saturated porous medium, while the piles were represented as concrete elements embedded in the soil, with pile–soil interaction included through interface contact to allow load transfer during mechanical loading and thermal expansion or contraction. The modelling procedure first established the initial stress condition, then applied the mechanical load to the pile heads, followed by time-dependent heating and cooling cycles applied to the energy piles. Three comparison cases with increasing levels of complexity were considered: a one-dimensional thermal consolidation problem, a full-scale single energy pile test, and a published energy pile group model. These cases were selected to evaluate the numerical implementation from a simple saturated porous medium response to more complex pile–soil interaction under thermal loading. In addition, mesh sensitivity, boundary effects, and numerical error sources were assessed to improve the reliability of the calculated settlement response and interaction factors.

Although additional experimental datasets would further strengthen the validation, particularly for unrestrained pile group settlement interaction, the selected cases assess the formulation from fundamental coupled THM behaviour to field-scale single-pile response and group-level pile–soil interaction.

3.6. Thermal consolidation verification

The first verification stage considered a one-dimensional thermal consolidation problem involving a fully saturated clay column. This case was selected because it represents a controlled coupled THM condition in which thermal loading generates pore-water pressure, subsequent drainage causes pore-pressure dissipation, and the soil undergoes time-dependent vertical deformation. Therefore, it provides a suitable basis for evaluating the hydraulic and thermal components of the formulation before applying the model to energy pile simulations.

The verification model consisted of a saturated clay column with a height of 7 m and a width of 2 m. A vertical surface traction of 1 kPa and a thermal load of 50 °C above the initial temperature were applied at the top boundary. A free-drainage boundary condition was assigned to the upper surface, while the lateral and bottom boundaries were treated as undrained. The material parameters adopted for the saturated clay column and water are summarised in Table 2. The model geometry, boundary conditions, and pore-pressure monitoring locations are shown in Fig. 2.

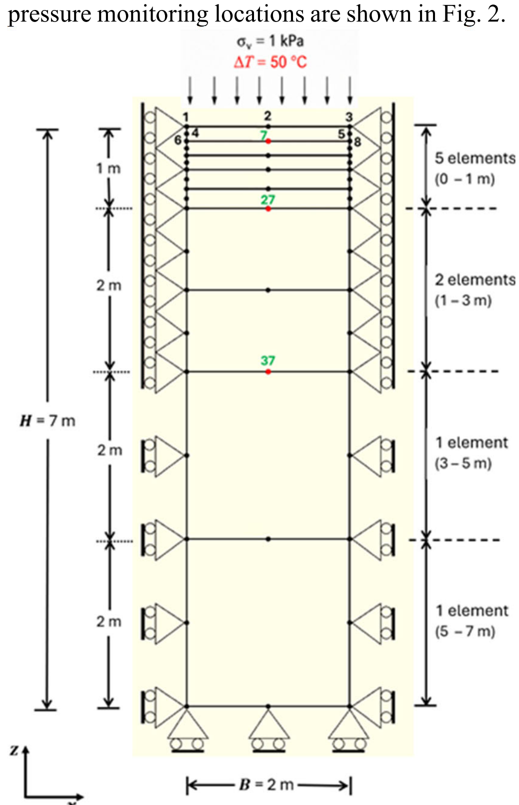

Fig. 2. Geometry, boundary conditions, mesh discretization, and pore-pressure monitoring nodes (7, 27, and 37) for the thermal consolidation verification model

The computed response was evaluated against previously published numerical solutions for the same thermal consolidation problem [42,43]. As shown in Fig. 3, the model captured both the time-dependent vertical deformation and the dissipation of excess pore-water pressure at the selected monitoring nodes. The predicted displacement response followed the same trend and comparable magnitude as the reference solutions, indicating that the model reproduced the coupled deformation of saturated clay under simultaneous mechanical and thermal loading. The pore-water pressure response at the selected monitoring nodes also showed good agreement with the comparison results. This verification step confirmed that the coupled formulation was capable of capturing the generation and dissipation of thermally induced excess pore pressure in saturated clay.

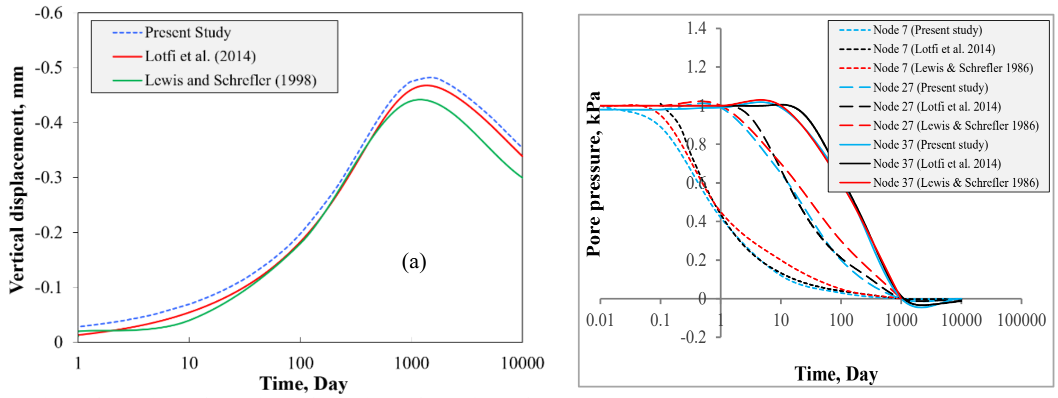

Fig. 3. Thermal consolidation verification: a vertical displacement–time response, b pore-water pressure dissipation at selected monitoring nodes

Table 2. Material input parameters adopted in the thermal consolidation verification

No.	Parameter group	Parameter [unit]	Symbol	Clay Soil	Water
1	Physical	Initial porosity [–]	n	0.2	-
2	Hydraulic	Soil intrinsic permeability [m^2]	K	46×10^{-18}	-
3	Hydraulic	Dynamic viscosity of pore water [Ns/m^2]	μ	-	0.001
4	Thermal	Coefficient of thermal conductivity [W/(m.C)]	λ	0.2	0.57
5	Thermal	Coefficient of thermal expansion [1/C]	α	9×10^{-7}	35×10^{-5}
6	Thermal	Specific heat capacity [J/(kg.C)]	C	732	4186

3.7. Full-scale single energy pile validation

The second stage involved validation against a full-scale single energy pile test of Bourne-Webb et al. [44]. This case was utilized to assess the ability of the numerical model to reproduce field-scale pile–soil interaction under combined mechanical and thermal loading.

Compared with the thermal consolidation problem, the single-pile case provides a more realistic assessment of pile-head displacement, axial force variation, and thermal stress development along the pile.

The simulated energy pile had a diameter of 0.55 m and a length of 23 m. The upper 4 m of the pile was installed in a granular soil layer, whereas the lower portion of the pile and the ground below the pile base were located in London clay. A mechanical load of 1200 kN was first applied to the pile head and then maintained during the heating and cooling stages. The adopted soil properties are summarized in Table 3.

Table 3. Input parameters assigned to the soil layers in the full-scale single energy pile validation model

No.	Parameter group	Parameter [unit]	Symbol	Granular soil	London clay
1	Physical	Unit weight [kN/m³]	γ	19	20
2	Mechanical	Elastic modulus [MPa]	E	20	800 S_u
3	Mechanical	Poisson's ratio [–]	ν	0.2	0.49
4	Strength	Friction angle [°]	ϕ	20	0
5	Strength	Cohesion [kN/m²]	c	0	70 + 7 z
6	Thermal	Coefficient of thermal expansion [1/K]	α	5.6×10^{-6}	1×10^{-5}
7	Thermal	Coefficient of thermal conductivity [W/(m.K)]	λ	2	1.5
8	Thermal	Specific heat capacity [J/(kg.K)]	C	1200	1000

Table 4. Mechanical, hydraulic, and thermal input parameters assigned to the soil and concrete in the energy pile group validation model

No.	Parameter	Parameter [unit]	Symbol	Soil	Concrete
1	Physical	Unit weight [kN/m³]	γ	20	25
2	Mechanical	Bulk modulus [MPa]	K	20	24510
3	Mechanical	Shear modulus [MPa]	G	12	9398
4	Hydraulic	Permeability coefficient [m/s]	k	1×10^{-8}	1×10^{-9}
5	Thermal	Coefficient of thermal expansion [1/K]	α	1×10^{-4}	1×10^{-5}
6	Thermal	Coefficient of thermal conductivity [W/(m.K)]	λ	1.7	1.8
7	Thermal	Specific heat capacity (J/(kg.K))	C	3034	880

The axial load distributions along the pile depth at the end of the cooling and heating phases are compared with the computed data in Fig. 4.
The predicted axial load profiles showed reasonable agreement with the reference response at the end of both cooling and heating.
In general, axial load decreased with depth, reflecting load transfer from the pile to the surrounding soil. Compared with the cooling phase, heating produced higher axial load in the upper part of the pile, indicating the effect of thermally induced expansion on the energy pile response.
Fig. 5 shows the load-displacement responses under mechanical loading only, mechanical loading with cooling, and mechanical loading with heating conditions.
The model reproduced the overall load-settlement trend under the different loading conditions, where axial load increased with pile-head settlement in all three cases.
These results indicate that the numerical model can reasonably capture the main thermo-mechanical mechanism controlling the response of a full-scale single energy pile.

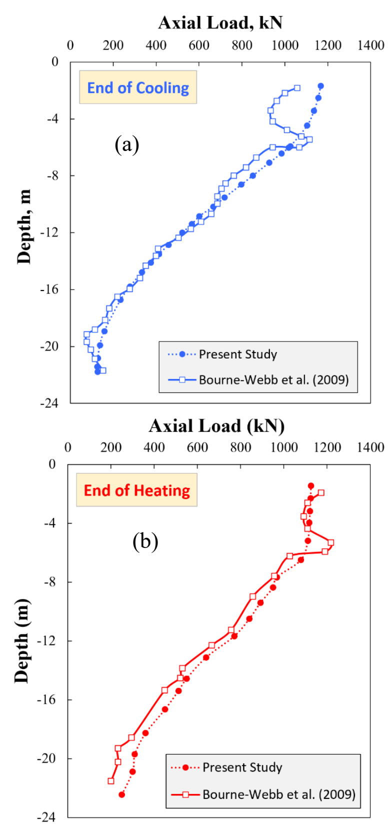

Fig. 4. Axial load distribution with depth at the end

of: a cooling, b heating

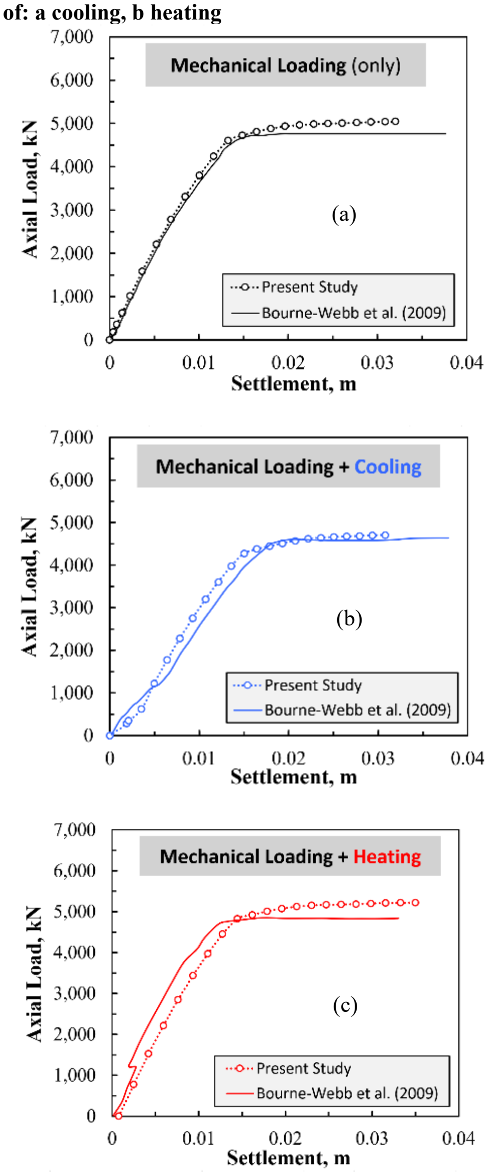

Fig. 5. Full-scale single energy pile validation based on axial load–settlement response under: a mechanical loading, b mechanical loading with cooling, c mechanical loading with heating

3.8. Full-scale single energy pile validation

The third stage considered validation against the published energy pile group model of Salciarini et al. [45].

This step was conducted because the present study focuses on settlement interaction between thermally active piles and adjacent structural piles, requiring the model to reproduce the coupled response of multiple piles interacting through saturated clay.

The reference case consisted of a 3 × 3 pile group with a 0.5 m thick rigid raft embedded in saturated clay and subjected to mechanical loading followed by cyclic thermal loading. The pile diameter and length were 0.6 m and 25 m, respectively. The soil properties, concrete properties, and thermal loading conditions were assigned consistently with the reference model, and the adopted input parameters are summarized in Table 4.

The numerical response was then assessed by comparing the predicted axial load and pore-pressure profiles with the published results of Salciarini et al. [45], as shown in Fig. 6.The comparison was made for the first thermal cycle, including the initial condition, 3 months of thermal loading, and 12 months, corresponding to the end of the first cycle. Fig. 6a compares the axial load distribution with depth for pile P5 at selected thermal loading stages, while Fig. 6b compares the pore-pressure distribution with depth for pile P9.

The predicted axial load profiles followed the same general trend as the reference results during thermal cycling, indicating that the model could reproduce axial load redistribution within the pile group.

The pore-pressure profiles also showed reasonable agreement with the published results, capturing the development of positive excess pore pressure during heating and its reduction or reversal during later stages of thermal loading. The apparent decrease in axial load between the initial condition and 3 months, followed by an increase toward 12 months, reflects the evolution of thermal load redistribution during the first heating–cooling cycle and is consistent with the selected comparison stages reported in the reference study.

Overall, the comparison confirms that the numerical model can reproduce the main coupled mechanisms involved in energy pile group behaviour, including thermal diffusion, pore-water pressure variation, and axial load redistribution.

This verification provides a basis for extending the model to the parametric investigation of unrestrained energy pile groups with different geometrical configurations.

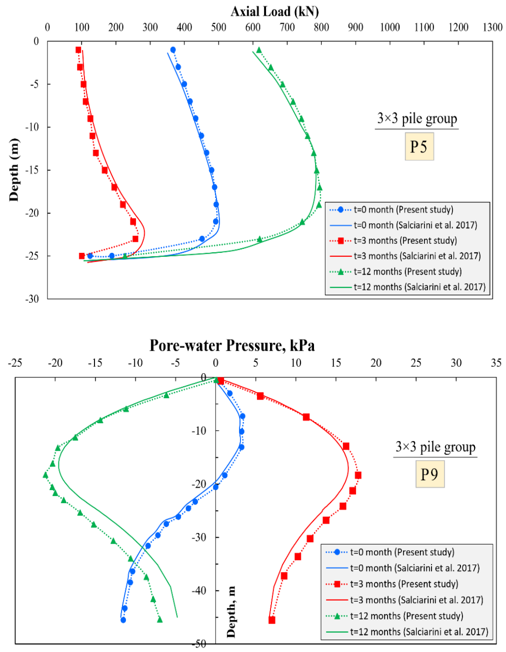

Fig. 6. Energy pile group response verification for the 3 × 3 pile group: a axial load distribution with depth for pile P5, b pore-water pressure distribution with depth for pile P9

3.9. Mesh sensitivity, boundary effects, and numerical error assessment

A numerical reliability assessment was conducted to reduce uncertainty associated with mesh discretization, model boundaries, and numerical approximation. This step is crucial because the interaction factor is calculated from pile displacement, and small numerical differences in settlement may influence the estimated pile-to-pile interaction.

The finite element mesh was refined around the piles, where the largest gradients in displacement, pore-water pressure, and temperature were expected. A gradually coarser mesh was used farther from the pile group to reduce computational cost while maintaining sufficient accuracy in the zone of interest. Mesh sensitivity was assessed by comparing pile-head displacement, excess pore-water pressure, and interaction factor for different mesh densities. The adopted mesh was considered suitable when further refinement produced only minor changes in the calculated response.

Boundary effects were evaluated by ensuring that the external boundaries were located sufficiently far from the pile group. This was necessary to prevent artificial restriction of displacement, pore-pressure dissipation, or thermal diffusion. The selected model dimensions were therefore evaluated to confirm that the response near the pile group was not significantly affected by the boundary location.

Potential numerical errors may arise from spatial discretisation, time-step size, convergence tolerance, interpolation of coupled field variables, and material idealisation. To minimise these effects, the thermal loading history was divided into appropriate time increments, convergence was monitored during each analysis step, and the same modelling procedure was used consistently across all parametric cases. Although these measures cannot eliminate all sources of uncertainty, they provide a consistent basis for comparing the influence of pile diameter, length, spacing, and group size on thermally induced settlement interaction.

4. Parametric study design

The verified numerical model was employed to conduct a parametric study on unrestrained energy pile groups embedded in saturated clay. The purpose of the parametric analysis was to evaluate how pile geometry, pile spacing, and group size influence thermally induced pile–soil–pile interaction under cyclic heating and cooling. Unlike capped or fixed-head pile groups, the pile heads were not restrained in the present simulations, enabling thermally induced displacement to develop more freely. This configuration was selected to isolate the interaction between thermally active piles and adjacent structural piles without the additional stiffness contribution of a raft, cap, or rigid superstructure.

4.1. Energy pile group geometry and configurations

Three free-head energy pile group arrangements were considered in the parametric study: 3 × 3, 4 × 4, and 5 × 5 groups, as illustrated in Fig. 7. In each arrangement, the corner piles were treated as thermally active energy piles, while the remaining piles were considered structural piles subjected only to mechanical loading. This configuration was adopted to investigate the influence of thermally active piles on adjacent structural piles through the surrounding saturated clay.

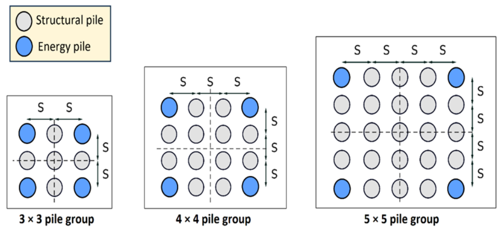

Fig. 7. Plan-view layouts of the three unrestrained energy pile groups

The finite element model had a height of 55 m and a width of 48 m to reduce boundary effects on the calculated displacement, pore-pressure, and temperature fields. The mesh was refined around the piles, where the highest gradients in stress, displacement, pore pressure, and temperature were expected, and became gradually coarser away from the pile group. For instance, Fig. 8 shows the three-dimensional model geometry and mesh refinement adopted for the representative 5 × 5 pile group model.

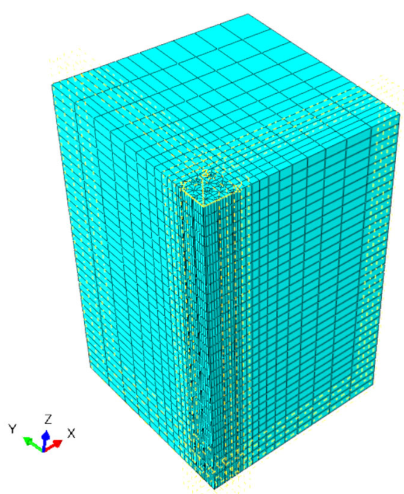

Fig. 8 Three-dimensional finite element mesh for the 5 × 5 energy pile group model

Pile length, diameter, and spacing were varied systematically to evaluate the effects of geometry on the interaction factor. Four pile lengths (L = 20, 25, 30, and 35 m), four pile diameters (D = 0.4, 0.6, 0.8, and 1 m), and two centre-to-centre pile spacings (S = 2 and 3 m) t were considered and compared. These variables were expressed using the spacing ratio (S/D) and slenderness ratio (L/D). The adopted pile geometries and material properties are summarized in Table 5.

4.2. Soil, pile, and interface properties

The soil was modelled as a homogeneous, isotropic, fully saturated clay layer. The groundwater table was assumed to be located at the ground surface, and the soil model was treated as saturated throughout the analysis. The clay behaviour was represented using the Mohr–Coulomb constitutive model. Although advanced thermo-elastoplastic models are available for saturated clay, the present study focused on moderate temperature variations, for which thermal yielding was not expected to dominate the response. Therefore, the adopted model was considered suitable for evaluating the serviceability-level interaction response of the pile groups. The clayey soil parameters assigned into the model for parametric study are summarized in Table 6.

The piles were modelled as concrete elements with linear elastic behaviour. Their mechanical, hydraulic, and thermal properties were kept constant throughout the parametric study to isolate the influence of geometry and group configuration. The pile–soil interface was represented using frictional contact, allowing shear transfer between the pile and surrounding clay during mechanical loading and thermal expansion or contraction. The interface friction coefficient was selected consistently with the friction angle assigned to the clay.

A vertical mechanical load of 540 kN was applied to the head of each pile to represent the structural load transferred from the superstructure. This load was maintained during the thermal cycles so that the additional pile response could be attributed to thermal loading and pile–soil–pile interaction. No pile-head restraint was applied in the main parametric models, which allowed the thermally induced displacement of the piles to be evaluated.

4.3. Heating–cooling thermal cycles

The entire soil–pile system was initially assigned a uniform temperature of 20 °C. Thermal loading was then applied to the energy piles to represent repeated seasonal heating and cooling cycles. The heat-exchanger pipes and circulation fluid were not explicitly modelled; instead, the temperature variation was applied directly and uniformly to the thermally active pile elements. This simplification was adopted because the study focused on pile group interaction rather than the detailed thermal performance of the heat-exchange system.

Table 5. Geometrical, mechanical, hydraulic, and thermal input parameters assigned to the piles in the parametric analyses.

No.	Parameter group	Parameter [unit]	Symbol	Value
1	Geometry	Pile length [m]	L	20, 25, 30, 35
2	Geometry	Pile diameter [m]	D	0.4, 0.6, 0.8, 1
3	Geometry	Pile spacing [m]	S	2, 3
4	Mechanical	Elastic modulus [MPa]	E	25000
5	Mechanical	Poisson's ratio [-]	ν	0.33
7	Hydraulic	Permeability coefficient [m/s]	k	1×10^{-9}
6	Thermal	coefficient of thermal expansion [1/K]	α	1×10^{-5}
8	Thermal	Specific heat capacity [J/(kg.K)]	C	880

Table 6. Clay soil input parameters adopted for the thermo-hydro-mechanical parametric models

No.	Parameter group	Parameter [unit]	Symbol	Value
1	Physical	Unit weight [kN/m^3]	γ	20
2	Mechanical	Elastic modulus [MPa]	E	30
3	Mechanical	Poisson's ratio [-]	ν	0.25
4	Hydraulic	Permeability coefficient [m/s]	k	1×10^{-8}
5	Strength	Friction angle [°]	ϕ	10
6	Strength	Cohesion [kPa]	c	Variable
7	Thermal	Coefficient of thermal expansion [1/K]	α	1×10^{-4}
8	Thermal	Coefficient of thermal conductivity [W/(m.K)]	λ	1.7
9	Thermal	Specific heat capacity [J/(kg.K)]	C	3034

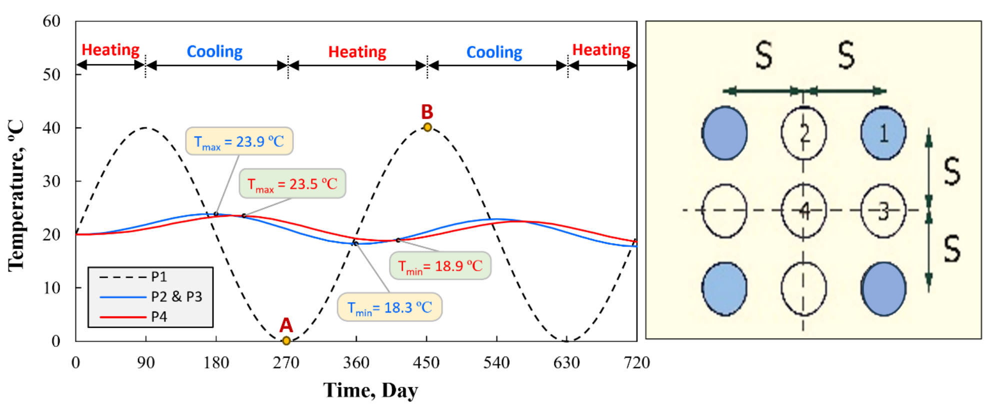

Fig. 9. Heating–cooling thermal cycle applied to the energy pile and induced temperature variations in adjacent structural piles

The applied thermal loading consisted of two complete heating–cooling cycles over a total duration of 720 days. The two-year thermal loading history was adopted for controlled parametric comparison and was not intended to represent long-term settlement, thermal accumulation, or fatigue behaviour over the full-service life of an energy pile system. The applied heating–cooling cycle and the induced temperature variations in the adjacent structural piles are shown in Fig. 9. In the first stage, the temperature of the energy piles was increased from 20 °C to 40 °C (over 90 days). The temperature was then reduced from 40 °C to 0 °C (over the following 180 days). In the second heating stage, the temperature was increased from 0 °C to 40 °C (over 180 days), followed by a second cooling phase from 40 °C to 0 °C (over another 180 days). Finally, the temperature was increased from 0 °C to 20 °C (over 90 days) to complete the two-year thermal loading history. The maximum induced temperatures in the adjacent structural piles remained limited to 18.3 °C and 23.9 °C, indicating that the thermal influence on non-active piles was relatively small. The temperature distribution around the pile groups was monitored at key stages of the thermal cycle, particularly at the end of the first cooling phase (Point A at day 270) and the end of the second heating phase (Point B at day 450). These stages were selected because they correspond to important thermal contraction and expansion conditions and were used to evaluate the phase-dependent interaction between energy piles and structural piles.

4.4. *Definition of interaction factor and response indices*

The interaction factor, defined previously in Eq. (1), was adopted as the main response index for quantifying thermally induced settlement interaction between energy piles and adjacent structural piles. In the present parametric study, this dimensionless parameter was calculated using the axial displacement induced in a structural pile by thermal loading of a nearby energy pile, normalized by the reference axial displacement of a single isolated pile under comparable conditions. This approach provides a practical basis for comparing pile–soil–pile interaction across different group geometries and thermal phases.

The interaction factor was evaluated at selected stages of the heating–cooling cycles, including the end of the first cooling phase (Point A in Fig. 9) and the end of the second heating phase (Point B in Fig. 9). These stages were selected to compare the influence of thermal contraction and expansion on the pile group response. In addition, the maximum interaction factor over the full 720-day loading period was recorded to identify the most critical serviceability condition.

In addition to the interaction factor, several response quantities were monitored to interpret the coupled THM behaviour of the energy pile groups. These included pile-head displacement, axial stress distribution along the energy piles, temperature variation in adjacent structural piles, and excess pore-water pressure in the surrounding clay. These response indices were used to clarify the mechanisms controlling settlement interaction, including thermal expansion during heating, thermal contraction during cooling, pore-water pressure generation and dissipation, and stress reversal in the energy piles.

The resulting numerical database was then utilized to examine the effects of spacing ratio, slenderness ratio, pile diameter, pile length, and group size on thermally induced settlement interaction. The same database also provided the basis for developing a simplified dimensionless expression for estimating the interaction factor in unrestrained energy pile groups.

5. Results

5.1. *Temperature transfer to adjacent structural piles*

The temperature field around the pile groups at the selected cooling and heating stages is shown in Fig. 10. The temperature disturbance was concentrated around the thermally active energy piles, while the temperature variation decreased with distance from the heat source. During the cooling phase, lower-temperature zones developed around the energy piles, whereas during the heating phase, higher-temperature zones expanded into the surrounding soil. The extent of the thermal influence zone varied with pile group size, but the temperature change in the adjacent structural piles remained relatively limited compared with the applied temperature variation in the energy piles.

This result indicates that the settlement interaction between energy piles and structural piles was not mainly controlled by direct heating or cooling of the structural piles. Instead, the interaction was governed primarily by thermal expansion or contraction of energy piles and the resulting displacement transfer through the surrounding saturated clay.

5.2. *Heating–cooling asymmetry in interaction factor*

The variation of interaction factor with normalized pile spacing (S/D) is shown in Fig. 11 for the various pile groups. The results demonstrate a clear difference between the heating and cooling phases. For all group sizes, the interaction factor was consistently higher at the end of the second heating phase (Point B in Fig. 9) than at the end of the first cooling phase (Point A in Fig. 9). This confirms that pile expansion during heating produced greater pile–soil–pile interaction than pile contraction during cooling.

During heating, the interaction factor was generally within the range of approximately 0.03–0.05, whereas during cooling it was much lower, approximately 0.005–0.02.

This indicates that the serviceability response of unrestrained energy pile groups is more critical during heating than cooling. The higher interaction factor during heating can be attributed to the outward expansion of the thermally active piles, which mobilizes stronger displacement transfer through the surrounding soil. The results also show that the interaction factor generally decreased as S/D increased. This trend confirms that greater pile spacing reduces thermal interaction between energy piles and adjacent structural piles.

Among the investigated group sizes, the 5 × 5 group generally produced the highest interaction factor during heating, indicating that pile group size can intensify the thermal interaction effect.

End of Cooling (A)

End of Heating (B)

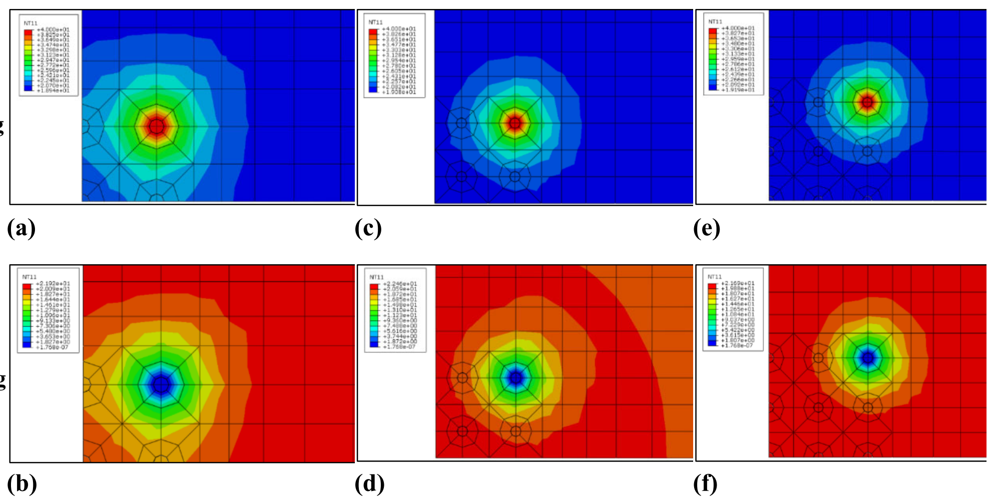

Fig. 10. Temperature distribution around the energy pile groups at selected thermal stages [Points A and B]: a-b 3 × 3 group [cooling at day 270, and heating at day 450], c-d 4 × 4 group [cooling at day 270, and heating at day 450], e-f 5 × 5 group [cooling at day 270, and heating at day 450]

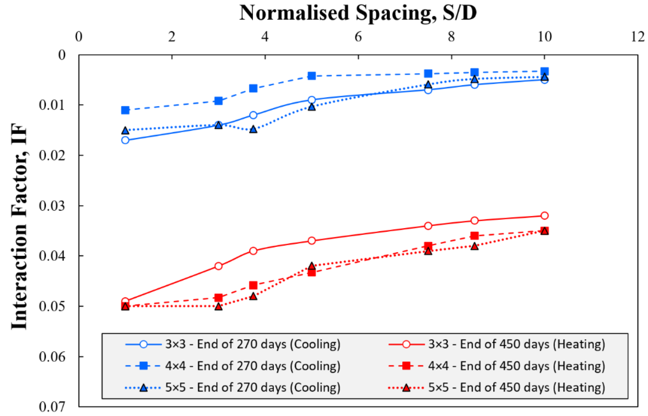

Fig. 11. Influence of normalized spacing (S/D) on the interaction factor for different energy pile groups under first-cooling and second-heating conditions

5.3. Effects of spacing, diameter, and slenderness ratio

The effects of spacing ratio and pile group size on the interaction factor are shown in Fig. 12. The results indicate that increasing the normalized spacing (S⁄D), reduced the interaction factor for all pile group configurations. This reduction was more evident at smaller spacing ratios, where the energy pile and structural piles were close enough for stronger displacement interaction to develop through the surrounding clay. At larger spacing ratios, the interaction factor gradually approached lower values, suggesting that the influence of thermal loading became less significant as the piles were separated further.

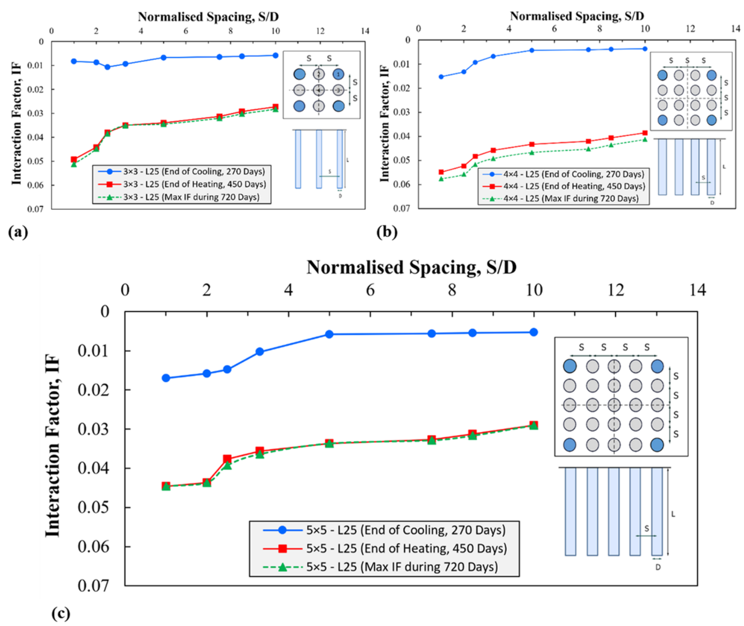

Fig. 12 Influence of normalized spacing (S/D) on the interaction factor for the three energy pile groups under: a cooling, b heating, c maximum-response conditions

Fig. 12 also compares the interaction factor at the end of cooling, at the end of heating, and at the maximum relative displacement over the full thermal loading period. The maximum interaction factor generally followed the heating response more closely than the cooling response, confirming that the most critical settlement interaction occurred during the expansion phase. This result is consistent with the heating–cooling asymmetry shown in Fig. 11.

Fig. 13 shows the effect of pile slenderness ratio (L/D). For both the 3 × 3 and 4 × 4 pile groups, the interaction factor decreased as L/D increased. This indicates that longer and more slender piles produced lower settlement interaction than shorter and larger-diameter piles. In contrast, piles with lower slenderness ratios generated stronger interaction because their greater diameter and lower relative length increased the influence of thermal expansion on the surrounding soil.

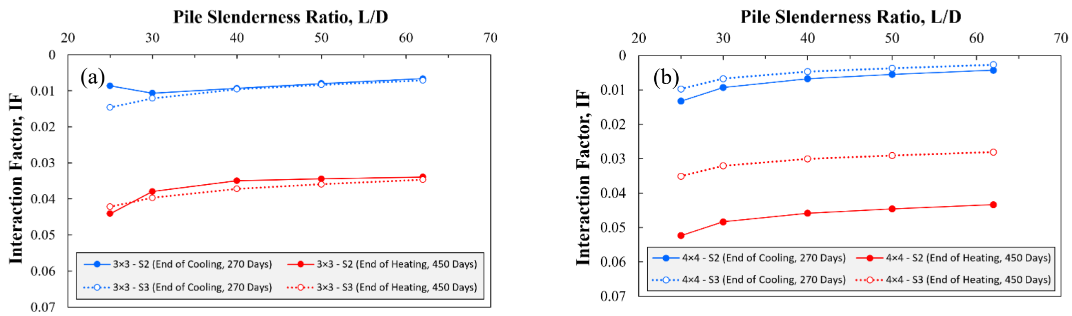

Fig. 13 Influence of pile slenderness ratio (L/D) on interaction factor for two pile spacings (S= 2 m and 3 m): a 3 × 3 energy pile group, b 4 × 4 energy pile group

The quantitative comparison indicates that the interaction factor was influenced by the combined effects of pile spacing, diameter, and length. Because changing pile diameter also changes both S/D and L/D, its effect should be interpreted together with the corresponding changes in normalised spacing and slenderness ratio. However, pile length and pile diameter showed contrasting effects on thermal interaction.

Under fixed spacing and diameter conditions (S = 2 m and D = 0.4 m), increasing pile length from 20 to 35 m reduced the interaction factor by approximately 61–68% during cooling and 47–52% during heating. In contrast, under fixed length and spacing conditions (S = 2 m and L = 25 m), increasing pile diameter from 0.4 to 1 m increased the heating-stage interaction factor by approximately 21–30%.

In sum, the results show that pile spacing, pile diameter, and pile slenderness are crucial geometrical controls on thermally induced interaction.

In general, larger pile spacing and higher slenderness ratios reduced the interaction factor, whereas larger pile diameters and larger group sizes increased the thermal influence on adjacent structural piles.

6. Simplified interaction-factor model

6.1. Dimensionless interaction-factor equation

The numerical results demonstrated that the interaction factor is mainly governed by pile spacing, pile slenderness, pile group size, thermal loading amplitude, and the phase of the thermal cycle. To provide a practical approach for preliminary assessment, a simplified dimensionless expression is proposed for estimating the interaction factor in unrestrained energy pile groups. The proposed expression relates the interaction factor to the main geometrical and thermal variables identified from the numerical modelling:

$$IF_\theta = A_\theta . G_n . \left(\frac{S}{D}\right)^{-m_\theta} . \left(\frac{L}{D}\right)^{-q_\theta} . \left(\frac{|\Delta T|}{20}\right) \quad (6)$$

where IF_θ is the interaction factor for thermal phase θ, S is the centre-to-centre pile spacing, D is the pile diameter, L is the pile length, and $|\Delta T|$ is the absolute temperature change relative to the reference temperature. The parameters A_θ, m_θ, q_θ, and r_θ are phase-dependent fitting coefficients calibrated separately for cooling, heating, and maximum-response conditions. The term G_n is a group-size modifier used to account for the influence of the number of piles in the group:

$$G_n = 1 + b_\theta . \left(\frac{N_p - 9}{16}\right) \quad (7)$$

where N_p is the total number of piles in the group, and b_θ is a phase-dependent coefficient. For the pile groups considered in this study, N_p equals 9, 16, and 25 for the 3 × 3, 4 × 4, and 5 × 5 configurations, respectively. This definition gives G_n = 1 for the 3 × 3 group and allows the group-size effect to increase progressively for larger pile groups.

The coefficients in Eqs. (6) and (7) were obtained by nonlinear regression of the numerical database. The calibrated coefficients are summarized in Table 7. In this formulation, A_θ controls the reference magnitude of the interaction factor, m_θ describes the influence of spacing ratio, q_θ describes the influence of slenderness ratio, r_θ accounts for the thermal loading amplitude, and b_θ represents the group-size effect. The proposed simplified interaction-factor model, defined by Eqs. (6) and (7), was calibrated and assessed using the full numerical database generated from the investigated pile group sizes, pile lengths, pile diameters, pile spacings, and thermal response conditions. Therefore, its performance should be interpreted based on its consistency across the complete dataset rather than from selected individual cases.

Table 7. Calibrated coefficients for the simplified interaction-factor model under heating and cooling phases

Thermal phase, θ	A_θ	m_θ	q_θ	r_θ	b_θ	Calibration basis
Cooling	0.0317	0.230	0.267	0	0.028	IF values at day 270
Heating	0.0552	0.138	0.0783	0	0.163	IF values at day 450
Maximum response	0.0516	0.180	0.0427	0	0.188	Maximum IF over 720 days

The coefficients were obtained from the interaction-factor values calculated for the 3 × 3, 4 × 4, and 5 × 5 pile groups. Since the calibration data were generated for a single thermal-amplitude level (ΔT = 20 ºC), the temperature-amplitude exponent r_θ was not independently identifiable and was fixed in the present calibration. Consequently, the calibrated coefficients should be applied only within the thermal loading range considered in this study.

The proposed expression is consistent with the overall trends observed in the numerical results. The spacing-ratio term captures the reduction in interaction factor with increasing pile spacing, while the slenderness-ratio term accounts for the influence of pile length and diameter. The group-size modifier reflects the greater thermal interaction observed in larger pile groups. Although the thermal-amplitude term is included to preserve generality, additional simulations with different temperature amplitudes are required before r_θ can be independently calibrated.

6.2. Calibration range and design application

The proposed expression is intended for preliminary serviceability assessment of thermally induced settlement interaction in unrestrained energy pile groups. It was developed based on the numerical database generated in this study and should be applied only within the range of the analyzed parameters. The calibration range includes 3 × 3, 4 × 4, and 5 × 5 pile groups, pile lengths of 20–35 m, pile diameters of 0.4–1 m, and pile spacings of 2–3 m. The simulations were conducted for saturated clay, unrestrained pile heads, and two heating–cooling cycles over 720 days.

For design use, the coefficients in Eqs. (6) and (7) should be calibrated separately for the heating and cooling phases because the numerical results showed a clear asymmetry between thermal expansion and contraction. Heating generally produced higher interaction factors than cooling, indicating that the heating phase is more critical for serviceability assessment. Therefore, when the objective is to obtain a conservative preliminary estimate, the heating-phase coefficients should be applied. In practical application, the coefficient can be used as an early-stage screening parameter to estimate whether thermal operation of energy piles is likely to cause additional settlement interaction in adjacent structural piles and to compare alternative pile spacing, length, diameter, and group-size arrangements before more detailed project-specific analysis is undertaken.

The proposed equation provides an interpretable preliminary estimation framework because each term has a clear physical meaning: S⁄D represents pile spacing effects, L⁄D represents pile slenderness effects, (|ΔT|)⁄20 represents normalized thermal loading amplitude, and G_n represents group-size influence. This makes the equation more suitable for engineering interpretation and preliminary comparison between alternative pile group configurations.

However, the equation should not be treated as a universal design equation. It is a calibrated numerical expression developed for the specific soil condition, boundary condition, and thermal loading history considered in this study. Its main value is to support early-stage serviceability assessment and to identify how changes in pile geometry and group size may influence thermally induced settlement interaction.

6.3. Limitations and future extension

The proposed model has several limitations that should be recognized before practical application. First, the equation was calibrated using numerical results for homogeneous, isotropic, fully saturated clay. Therefore, it should not be directly applied to layered soils, unsaturated soils, anisotropic deposits, or soils with significant creep, cracking, or thermal hardening/softening without further validation.

Second, the pile heads were assumed to be unrestrained in the parametric models. This condition was intentionally selected to isolate pile–soil–pile interaction caused by thermal loading. However, many practical foundation systems include pile caps, rafts, or superstructure restraint, which can significantly alter axial stress development and pile-head displacement. Additional calibration is therefore required before the equation can be used for restrained, capped, or piled-raft systems.

Third, the thermal loading was idealized as regular heating–cooling cycles over 720 days. Real energy pile systems may experience irregular thermal demand, different heating and cooling amplitudes, potential long-term thermal accumulation, seasonal drift, and groundwater-induced heat transport. These effects are not explicitly captured in the present equation. In addition, uncertainty in groundwater conditions, seasonal thermal demand, and long-term thermal drift may influence the predicted settlement response; therefore, future extensions should consider uncertainty-based assessment approaches, such as recent groundwater-related uncertainty quantification methods, to improve reliability for practical applications.

Fourth, the equation is based on a limited range of pile group geometries. Although 3 × 3, 4 × 4, and 5 × 5 arrangements were considered, irregular pile layouts, mixed pile diameters, variable pile lengths, and non-symmetric locations of energy piles were not included. Future studies may expand the database to include these conditions and refine the group-size modifier.

Fifth, the proposed framework is intended for preliminary serviceability evaluation of thermally induced settlement interaction and should not be considered a substitute for project-specific structural capacity design. Such design should account for uncertainty in material strength and stiffness, construction details, structural capacity requirements, and relevant safety factors.

Finally, further validation against field measurements of adjacent pile settlement would strengthen the proposed approach. The present model was verified against published numerical results and full-scale single-pile responses; however, direct field measurements of settlement interaction in energy pile groups remain limited. Future work may combine numerical modelling, field monitoring, and uncertainty analysis to improve the reliability and general applicability of the proposed interaction-factor model.

7. Discussions

The results indicate that the response of unrestrained energy pile groups is strongly phase-dependent. Heating produced larger interaction factors than cooling, demonstrating that thermal expansion of the energy piles is the dominant mechanism controlling settlement interaction with adjacent structural piles. Although cooling generated lower interaction factors, it remained important since it produced tensile stress development within the energy piles. Therefore, serviceability assessment should consider both thermal phases: heating for settlement interaction and cooling for possible tensile stress demand.

Pile geometry had a significant influence on the generated interaction-factors. Increasing pile spacing reduced pile-to-pile interaction as the displacement influence zone around the thermally active piles became less significant at greater distances. In contrast, larger pile diameters increased the interaction factor, while longer piles generally reduced it. This indicates that pile slenderness is an important design parameter: short, large-diameter piles are more likely to transfer thermally induced displacement to the surrounding soil, whereas longer, more slender piles reduce this interaction effect. The results also showed that larger pile groups produced greater thermal interaction, especially during heating, suggesting that group size should be considered in serviceability-based design rather than treating energy piles as isolated elements. This extends previous interaction-factor interpretations by showing that, under unrestrained THM conditions, pile-to-pile interaction is not controlled by spacing alone, but also by pile slenderness, group size, and thermal phase.

The free-head condition adopted in this study should be considered when interpreting the results. Since no pile cap, raft, or superstructure restraint was included, thermally induced pile-head movement was allowed to develop more freely. As a result, the calculated interaction factors represent an unrestrained or weakly restrained condition. In practice, restrained pile groups may experience smaller pile-head displacements but larger thermally induced axial stresses. Therefore, the proposed interaction-factor model should not be directly applied to fixed-head or capped pile groups without additional calibration.

The simplified dimensionless interaction-factor equation proposed in this study provides a practical method for preliminary assessment of thermally induced settlement interaction. Its main advantage is that it relates the interaction factor to physically meaningful parameters, including spacing ratio, slenderness ratio, group size, and thermal phase. Compared with previous interaction-factor studies, the present work retains the practical advantage of a simplified formulation while focusing specifically on unrestrained energy pile groups and explicitly separating the heating and cooling responses. This makes it more suitable for early-stage comparison of pile group configurations. However, it should be employed as a screening approach rather than a final design equation, particularly for projects involving complex ground conditions or high serviceability sensitivity. The main limitations of this study are related to the idealized numerical conditions. The analyses were performed for homogeneous, isotropic, fully saturated clay and regular 3 × 3 to 5 × 5 pile group configurations. The thermal loading was represented by two regular heating–cooling cycles over 720 days, while real energy pile systems may experience irregular thermal demand, potential long-term thermal accumulation, seasonal drift, and variable groundwater conditions. Soil layering, anisotropy, creep, cracking, unsaturated behaviour, freezing–thawing effects, and field-measured adjacent pile settlements were not explicitly considered. Future work should extend the calibration database to different soil types, restraint conditions, pile arrangements, and extended or irregular operational conditions, supported where possible by field monitoring of energy pile groups.

8. Conclusions

This study investigated the thermo-hydro-mechanical response of unrestrained energy pile groups embedded in saturated clay, with emphasis on the interaction factor between thermally active piles and adjacent structural piles. Based on the numerical results, the following conclusions can be drawn:

1. The interaction factor was substantially dependent on the thermal phase. Heating produced higher interaction factors than cooling, indicating that thermal expansion of energy piles governed the maximum settlement interaction.

2. The computed interaction factor was consistently higher during heating than cooling, with values generally ranging from 0.03 to 0.05 during heating and 0.005 to 0.02 during cooling. This difference indicates that the heating phase should be regarded as the governing condition for thermally induced settlement interaction.

3. The interaction factor response was affected by the combined influence of pile spacing, diameter, length and thermal phase. Although greater pile spacing predictably reduced pile-to-pile interaction, the magnitude of this reduction depended on the accompanying pile geometry and heating–cooling condition. Under fixed spacing and diameter conditions, increasing pile length from 20 to 35 m led to reductions of approximately 61–68% during cooling and 47–52% during heating, confirming that longer piles can reduce thermally induced settlement interaction.

4. Larger pile groups produced greater thermal interaction, particularly during heating. Among

the investigated configurations, the 5 × 5 group generally showed the highest interaction factor.

5. A simplified dimensionless interaction-factor equation was proposed using spacing ratio, slenderness ratio, group size, and thermal phase. This relationship was derived from the numerical database developed in this study and should be interpreted as a preliminary estimation approach only within the investigated calibration range and modelling assumptions, including saturated clay, regular pile group configurations, unrestrained pile heads, and the applied two-year thermal loading history.

6. The proposed model is limited to homogeneous saturated clay, regular pile group configurations, unrestrained pile heads, and the applied two-year thermal loading history. Further validation is required for layered soils, other soil types, restrained pile groups, irregular thermal loading, and field-measured adjacent pile settlements.

Finally, the findings highlight that pile spacing, slenderness ratio, group size, and thermal phase should be explicitly considered when evaluating settlement interaction in unrestrained energy pile groups. In particular, the results show that thermally induced interaction is not governed solely by pile geometry; it also depends on the heating–cooling response of the pile–soil system. Therefore, serviceability assessment should account for both the maximum settlement interaction during heating and the stress reversal that may occur during cooling. The simplified interaction-factor approach proposed in this study provides a practical basis for preliminary comparison of pile group configurations within the investigated calibration range.

Conflict of interest

On behalf of all authors, the corresponding author states that there is no conflict of interest.

References

[1] Zhou, J., Zhang, Rh., Yu, Jl., Jin Sh (2026) Field study on heat transfer performance and thermo-mechanical properties of pre-bored PHC energy pile. Sci Rep 16: 7781. https://doi.org/10.1038/s41598-026-37817-z.

[2] Dehghan Haddad E, Janalizadeh Choobbasti A, Ghasemi Fare O (2024) Laboratory and numerical study of energy pile behavior under different thermal loading. Innov Infrastruct Solut 9: 190. https://doi.org/10.1007/s41062-024-01503-8.

[3] Azhar M, Yadav S, Mondal S, Sharma V (2024) Numerical investigation on the thermo-mechanical response of geothermal energy pile in East Indian climatic condition. Int J Civ Eng 22: 2147–2165. https://doi.org/10.1007/s40999-024-01012-w.

[4] Amirdehi HA, Shooshpasha I (2023) Contributions of constraints to mechanical fields of energy pile foundation. Innov Infrastruct Solut 8: 153. https://doi.org/10.1007/s41062-023-01115-8.

[5] Saggu R, Chakraborty T (2016) Thermomechanical response of geothermal energy pile groups in sand. Int J Geomech 16(4): 04015100. https://doi.org/10.1061/(ASCE)GM.1943-5622.0000567.

[6] Ghasemzadeh H, Aliverdi A. (2026) Energy piles: behavior and geoenvironmental challenges. Geomechanics and Geoenergy Journal, 8(4), pp. 75-97. https://doi.org/10.22107/ggj.2026.596200.127.

[7] Fang J, Feng S, Zhao Y, Zhang Z, Chen H (2025) Effects of thermohydromechanical response at the soil–pile interface on the bearing performance of energy piles. J Geotech Geoenviron Eng 151(1): 04024143. https://doi.org/10.1061/JGGEFK.GTENG-12464.

[8] Rafai M, Salciarini D, Vardon PJ (2025) Energy pile displacements due to cyclic thermal loading at different mechanical load levels. Acta Geotech 20(6): 3067–3086. https://doi.org/10.1007/s11440-025-02556-4.

[9] Rotta Loria A, Laloui L (2016) The interaction factor method for energy pile groups. Comput Geotech 80: 121–137. https://doi.org/10.1016/j.compgeo.2016.07.002.

[10] Rotta Loria AF, Laloui L (2017) Thermally induced group effects among energy piles. Géotechnique 67(5): 374–393. https://doi.org/10.1680/jgeot.16.P.039.

[11] Cesaro R, Di Laora R, Iodice C, Mandolini A (2024) Interaction domains for capacity-

and performance-based design of pile groups. Acta Geotech 19: 4695–4714. https://doi.org/10.1007/s11440-023-02168-w.

[12] Di Donna A, Rotta Loria AF, Laloui L (2016) Numerical study of the response of a group of energy piles under different combinations of thermo-mechanical loads. Comput Geotech 72: 126–142. https://doi.org/10.1016/j.compgeo.2015.10.023.

[13] Qiu C, Vasilescu R, Doghman M, Mroueh H, Bourne-Webb PJ (2025) Long-term thermo-mechanical behaviour of an energy pile installed in clay: field experiments and numerical simulations. Energy Build 349: 116498. https://doi.org/10.1016/j.enbuild.2025.116498.

[14] Liu M, Wang R, Zhou Y (2025) Numerical study on the thermo-hydro-mechanical behavior of energy micropiles in hypoplastic soft clay under cyclic thermal loading. Int J Numer Anal Methods Geomech 49(12): 2731–2748. https://doi.org/10.1002/nag.4007.

[15] Ghorbani A, Zhang C, Li X (2026) Numerical study of energy piles in unsaturated soils. Comput Geotech 178: 106845. https://doi.org/10.1016/j.compgeo.2025.106845.

[16] Di Donna A, Laloui L (2015) Numerical analysis of the geotechnical behaviour of energy piles. Int J Numer Anal Methods Geomech 39(8): 861–888. https://doi.org/10.1002/nag.2341.

[17] Ding X, Zhang D, Wang C, Bouazza A, Kong G (2023) Thermally induced mechanical interactions of energy pile groups subjected to cyclic nonsymmetrical thermal loading. Comput Geotech 162: 105705. https://doi.org/10.1016/j.compgeo.2023.105705.

[18] Wang ZJ, Fang PF, Zhang RH, Wang KH, Xie XY (2019) FEM analysis and simplified approach for a single energy pile subjected to thermo-mechanical loads. Math Probl Eng 2019: 2098350. https://doi.org/10.1155/2019/2098350.

[19] Murphy KD, McCartney JS, Henry KS (2015) Evaluation of thermo-mechanical and thermal behavior of full-scale energy foundations. Acta Geotech 10(2): 179–195. https://doi.org/10.1007/s11440-013-0298-4.

[20] Loveridge FA, Powrie W (2013) Pile heat exchangers: thermal behaviour and interactions. Proc Inst Civ Eng Geotech Eng 166(2): 178–196. https://doi.org/10.1680/geng.10.00098.

[21] Al-Defae A, Al-Rubaye A, Hytiris N, Jefferson I, Chapman DN, Faramarzi A (2024) Full-scale in-situ tests on a displacement cast in situ energy pile: effects of cyclic thermal loads under different mechanical load levels on pile stress and strain. Geomech Energy Environ 40: 100606. https://doi.org/10.1016/j.gete.2024.100606.

[22] Coccia CJR, McCartney JS (2016) Thermally induced pore water pressures, strains, and preconsolidation pressure of compacted clay. J Geotech Geoenviron Eng 142(10): 04016057. https://doi.org/10.1061/(ASCE)GT.1943-5606.0001522.

[23] Cekerevac C, Laloui L (2004) Experimental study of thermal effects on the mechanical behaviour of a clay. Int J Numer Anal Methods Geomech 28(3): 209–228. https://doi.org/10.1002/nag.332.

[24] Sani AK, Singh RM, Amis T, Cavarretta I (2013) A review on the performance of geothermal energy pile foundation, its design process and applications. Renew Sustain Energy Rev 24: 450–460. https://doi.org/10.1016/j.rser.2013.03.040.

[25] Mirfallah Lialestani SP, Parcerisa D, Himi M, Shahri AA (2024) A novel modified bat algorithm to improve the spatial geothermal mapping using discrete geodata in Catalonia-Spain. Model Earth Syst Environ 10: 4415–4428. https://doi.org/10.1007/s40808-024-01992-7.

[26] Shahri AA, Shan C, Larsson S (2022) A novel approach to uncertainty quantification in groundwater table modeling by automated predictive deep learning. Nat Resour Res 31(3): 1907–1924. https://doi.org/10.1007/s11053-022-10051-w.

[27] Mirfallah Lialestani SP, Parcerisa D, Himi M, Shahri AA (2022) Generating 3D geothermal maps in Catalonia, Spain using a

hybrid adaptive multitask deep learning procedure. Energies 15: 4602. https://doi.org/10.3390/en15134602.

[28] Poulos HG, Davis EH (1980) Pile foundation analysis and design. Wiley, New York.

[29] Abdel-Azim OA, Abdel-Rahman K, El-Mossallamy YM (2020) Numerical investigation of optimized piled raft foundation for high-rise building in Germany. Innov Infrastruct Solut 5: 11. https://doi.org/10.1007/s41062-019-0258-4.

[30] Shaaban MGI, Kenawi MA, Senoon AA, Abd El-Naiem MA (2023) Effects of excavation and construction sequence on behavior of existing pile groups. Innov Infrastruct Solut 8: 223. https://doi.org/10.1007/s41062-023-01193-8.

[31] Mylonakis G, Gazetas G (1998) Settlement and additional internal forces of grouped piles in layered soil. Géotechnique 48(1): 55–72. https://doi.org/10.1680/geot.1998.48.1.55.

[32] Sailer C, Koppel A, Adam D (2012) Thermally induced interaction effects in energy pile groups. Acta Geotech 7(2): 109–124. https://doi.org/10.1007/s11440-012-0152-3.

[33] Park S, Lee SR, Nguyen T (2013) Thermo-mechanical interaction behavior of energy pile groups using interaction factors. Comput Geotech 49: 1–12. https://doi.org/10.1016/j.compgeo.2012.09.006

[34] Wang C, Zhang D, Li X, Liu H (2024) Thermomechanical analysis of energy piles using a load-transfer approach considering soil coupling effects. Comput Geotech 168: 106147. https://doi.org/10.1016/j.compgeo.2024.106147.

[35] Liu C, Li J, Zhou P, Liu G, Li P (2025) Thermo-hydro-mechanical behavior of energy piles in partially saturated soils: a theoretical prediction approach. Comput Geotech 185: 107332. https://doi.org/10.1016/j.compgeo.2025.107332.

[36] Huang L, Ding Z, Song C (2025) A novel three-dimensional analytical model for the thermomechanical responses of energy piles and the surrounding soil based on thermoelastic theory. Int J Numer Anal Methods Geomech 49(12): 2749–2762. https://doi.org/10.1002/nag.4010.

[37] Rafai M, Tafili M, Dong Y, Vardon PJ (2026) Thermo-plastic response of energy piles during long-term monotonic cooling. Comput Geotech 191: 107839. https://doi.org/10.1016/j.compgeo.2025.107839.

[38] Al-Khoury R, Bonnier PG (2006) Efficient finite element formulation for geothermal heating systems. Part II: transient analysis. Int J Numer Methods Eng 67(5): 725–745. https://doi.org/10.1002/nme.1650.

[39] Cui C, Liu Z, Liu J, You Y (2025) Thermo-mechanical coupling model for energy piles: dynamic interface behavior and sustainable design implications. Buildings 15(21): 3984. https://doi.org/10.3390/buildings15213984.

[40] Dassault Systèmes SIMULIA (2013) Abaqus 6.13 documentation (User's Guide and Analysis User's Guide). SIMULIA, RI.

[41] Sadrjamali M, Hamidi A (2025) The use of interaction factor for analysis of energy pile groups without head restraints. Geomech Geoeng 20(4): 687–706. https://doi.org/10.1080/17486025.2024.2439431.

[42] Lewis RW, Schrefler BA (1998) The finite element method in the static and dynamic deformation and consolidation of porous media. John Wiley & Sons, Chichester.

[43] Lotfi E, Delfan S, Hamidi A, Shahir H, Asadollahfardi G (2014) A numerical approach for one-dimensional thermal consolidation of clays. Int J Civ Eng 12(1): 85–91.

[44] Bourne-Webb PJ, Amatya B, Soga K, Amis T, et al. (2009) Energy pile test at Lambeth College, London: geotechnical and thermodynamic aspects of pile response to heat cycles. Géotechnique 59(3): 237–248. https://doi.org/10.1680/geot.2009.59.3.237.

[45] Salciarini D, Ronchi F, Tamagnini C (2017) Thermo-hydro-mechanical response of a large piled raft equipped with energy piles: a parametric study. Acta Geotech 12: 703–728. https://doi.org/10.1007/s11440-016-0463-6